Coherent control of two-photon absorption of Pr³⁺ ion by shaped ultrashort laser pulses

Wenjing Cheng (程文静), Shian Zhang (张诗按), Tianqing Jia (贾天卿)*,
Jing Ma (马　婧), Donghai Feng (冯东海), and Zhenrong Sun (孙真荣)

State Key Laboratory of Precision Spectroscopy, Department of Physics,
East China Normal University, Shanghai 200062, China
*Corresponding author: tqjia@phy.ecnu.edu.cn

Enhancing the photoluminescence and depressing the background emission are important problems in rare earth ion-doped materials. In this letter, the two-photon absorption (TPA) probability in a Pr³⁺ ion system is enhanced by a factor of 12.3 by a π-phase step scanning of ultrashort laser pulses. This level is significantly higher than that achieved by a transform-limit pulse. However, the laser intensity of shaped pulse is reduced to 37% of the initial transform-limited pulse. In this method, the TPA probability can also be reduced to 58%. Furthermore, the effect of the shift of the intermediate energy level and the bandwidth of final states on TPA probability is discussed.

OCIS codes: 190.4180, 190.7110, 320.5540, 190.7220.
doi: 10.3788/COL201311.041903.

Upconversion luminescence (UCL) of lanthanide ion-doped materials is an active research field for the applications in biological labeling, light emitting displays, optical data storage, and solid-state lasers[1−5]. In recent years, Pr³⁺ ions have attracted considerable attention because of their fluorescence features of upconversion and ultraviolet (UV) emission. The energy level structure of Pr³⁺ ions allows many linear and non-linear effects, such as UV tunable luminescence from 4f5d states[6], green and red emission from ³P₀ or ¹D₂ states[7−9], and photon cascade emissions[10].

Enhancing UCL is an important problem. As the concentration of Pr³⁺ ions is increased within the range of 0 to 3 mol%, the method intensity from ³P₀ states also increases. However, this fluorescence intensity decreases as the concentration is further increased for concentration quenching[11]. Yb³⁺ ions are usually co-doped with Pr³⁺ ions as sensitizers to improve UCL for energy transferring excitation[12]. As the sample temperature is increased, the blue emission peaked at 485 nm evidently increases in Pr³⁺/Yb³⁺ co-doped fluoroindate glasses for the multiphonon-assisted anti-Stokes excitation of Yb³⁺ sensitizers and excited-state absorption of Pr³⁺ ions[13]. Coherent control is an efficient method of enhancing or cancelling specific multiphoton processes through quantum interference. Several theoretical studies exist on the applications of coherent control in the fields of molecular alignment and Raman scattering[14−17]. In the past decade, great advances were achieved in ultrafast laser, pulse-shaper, and optical parametric amplifier technology. Ultrashort laser pulses in the range of 260 to 1 600 nm can now be changed into an arbitrary temporal shape by manipulating the spectral phase and amplitude[18]. Recently, pulse shaping and coherent control have successful applications in various non-linear optical processes, such as photochemical reactions, multiphoton absorption, and coherent anti-Stokes Raman spectroscopy[16,17,19−21]. Meshulach *et al.* demonstrated that the non-resonant two-photon absorption (TPA) in a two-level system could be reduced or annihilated com-

pletely by manipulating the spectral phase of femtosecond laser pulses[20]. In a previous study, the resonant TPA in Rb vapor was enhanced by a factor of 7, but the peak intensity of the laser pulse was evidently reduced[21]. As pointed in Ref. [22], understanding the photophysical and photochemical quantum processes and providing effective control systems for these processes in condensed matters are important directions of quantum control.

In this letter, the coherent enhancement of the resonant TPA in a three-energy-level Pr³⁺ ion system is theoretically investigated by modulating the spectral phase of a femtosecond laser. The TPA probability is enhanced by a factor of 12.3 by a π-phase modulation because of the establishment of constructive interference. However, the laser intensity of the shaped pulse is reduced to 37% of the initial transform-limited (TL) pulse. A Pr³⁺ ion is considered to have an absorption bandwidth to investigate further the TPA of a Pr³⁺ ion doped in a crystal. The effective coherent feature is greatly influenced by the absorption bandwidth and the shift of intermediate energy level.

Considering the TPA in an atomic system excited by femtosecond laser pulses with electric field $E(t)$, the TPA probability is predicted by second-order time-dependent perturbation theory[20]:

$$P_f(t) \propto \left| -\frac{1}{\hbar^2}\mu_{ig}\mu_{fi} \int_{-\infty}^{t_2}\int_{-\infty}^{t_1} E(t_1)E(t_2) \right.$$
$$\left. \cdot \exp(j\omega_{fi}t_1)\exp(j\omega_{ig}t_2)\mathrm{d}t_2\mathrm{d}t_1 \right|^2, \qquad (1)$$

where μ_{ig} and μ_{fi} are the dipole moment matrix elements, $|g\rangle$, $|i\rangle$, and $|f\rangle$ are the ground, intermediate, and final energy levels, respectively, and ω_{ig}, ω_{fg}, and $\omega_{fg} - \omega_{ig} = \omega_{fi}$ are resonant frequencies for $|g\rangle \to |i\rangle$, $|g\rangle \to |f\rangle$, and $|i\rangle \to |f\rangle$, respectively.

For a resonant TPA in a three-level atomic system, the intermediate energy level is within the spectral range of the laser pulse. Transforming Eq. (1) into the frequency domain, the probability of final state $|f\rangle$ is approximated

by[21]

$$P_f \propto \left| -\frac{1}{ih^2}\mu_{ig}\mu_{fi}\left[i\pi E(\omega_{ig})E(\omega_{fg}-\omega_{ig})\right.\right.$$

$$\left.\left. + \mathfrak{G}\int_{-\infty}^{\infty}\frac{E(\omega)E(\omega_{fg}-\omega)}{\omega_{ig}-\omega}\right]d\omega\right|^2, \quad (2)$$

where $\mathfrak{G}$ is the principal value of Cauchy. $E(\omega)$ is the Fourier transform of laser field $E(t)$, $E(\omega) = A(\omega)\exp[i\Phi(\omega)]$, where $A(\omega)$ and $\Phi(\omega)$ are the spectral amplitude and phase, respectively. The first term in Eq. (2) is an on-resonant part that depends only on the spectral components at resonant frequencies. The second term is a near-resonant part that integrates over the contributions of all other spectral components. Therefore, the total TPA probability depends on the pathway interference of the on-resonant and near-resonant two-photon excitation. For TL pulses, the contributions coming from the frequency components $\omega > \omega_{ig}$ and $\omega < \omega_{ig}$ are easily verified as negative and positive, respectively. The summation of these two components is the destructive interference.

Preventing the destructive interference by a π-phase modulation is a simple way of enhancing the transition probability; however, this prevention reduces the laser intensity of the shaped pulse. Applying a π-phase modulation inverts the sign of $E(\omega)E(\omega_{fg}-\omega)$ in the near-resonant part, so that the near-resonant pathways interfere constructively.

The energy levels of a Pr^{3+} ion and a Pr^{3+} ion in a crystal are shown in Fig. 1. The electrons in the ground state $^3H_4$ can be excited to the final state $^3P_0$ via the intermediate state $^1G_4$ irradiated by femtosecond laser pulses, leading to the major emission from the $^3P_0$ state. The resonant transition frequencies of $^3H_4 \rightarrow{}^1 G_4$, $^1G_4 \rightarrow{}^3 P_0$, and $^3H_4 \rightarrow{}^3 P_0$ are $\omega_{ig} = 9\ 885$ cm^{-1}, $\omega_{fi} = 10\ 821$ cm^{-1}, and $\omega_{fg} = 20\ 706$ cm^{-1}, respectively. In the following calculation, the laser central frequency is set at 10 353 cm^{-1}, and the full width at half maximum is 1 200 cm^{-1} (Fig. 2(a)). The spectral resolution is set as 1 cm^{-1} (0.0933 nm), which is attainable in the experiment.

As shown in Fig. 2(a), π-phase modulation indicates that the spectral phase is π for all frequencies smaller than the phase step position and is zero for all larger frequencies. As shown in Fig. 2(b), the TL Gaussian pulses transform into double-humped pulses by π-step scanning from low to high frequency. The laser intensity of the shaped pulse with step position at 9885 is reduced
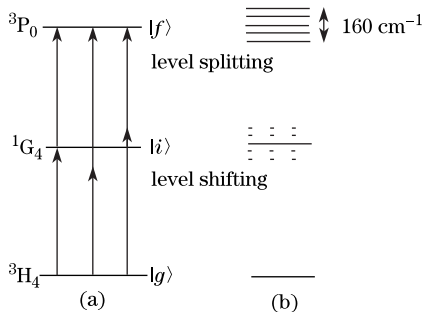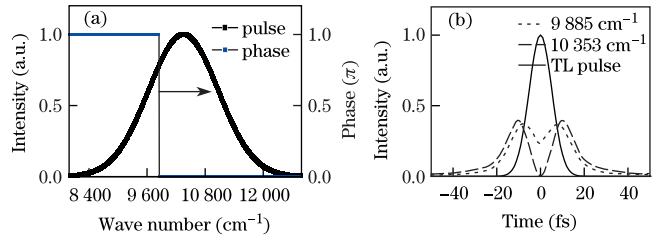

Fig. 2. (Color online) (a) Laser pulse with a π-phase step (blue line). (b) Temporal distribution of laser intensity with a π-phase modulation at the resonant frequency (red line) and central frequency (blue line). The black line is the initial TL pulse.

to 37% of the initial TL pulse. However, the simple phase modulation affects neither the pulse energy nor the power spectrum.

TPA probability is calculated as a function of the π-phase step position, as presented in Fig. 3. Figure 3 also presents the corresponding values of on-resonant and near-resonant probabilities. These results are normalized by the TPA probability excited by the TL pulse. When the phase step position is far from the resonant frequency, the absolute value of $1/(\omega_{ig}-\omega)$ is relatively small, as shown in Eq. (2). The sign of $E(\omega)E(\omega_{fg}-\omega)$ is inverted at a small part of the spectral components. Therefore, π-phase shaping has a slight effect on near-resonant TPA probability. However, when the phase step is at the resonant frequency of $\omega_{ig} = 9\ 885$ cm^{-1} or $\omega_{fi} = 10\ 821$ cm^{-1}, π-phase modulation inverts the sign of $E(\omega)E(\omega_{fg}-\omega)$ for $\omega < \omega_{ig}$ or $\omega > \omega_{fi}$, respectively. Moreover, the $|1/(\omega_{ig}-\omega)|$ factor is relatively large, and its sign is changed correspondingly. A completely constructive interference of all near-resonant TPA pathways is realized. The TPA probability enhances rapidly, and the enhancement factor reaches 12.3, whereas the laser intensity of the shaped pulse is reduced to 37% of the initial TL pulse.

In the phase step position at a frequency of 10 155 or 10 550 cm^{-1}, the near-resonant probability decreases to zero for the destructive interference, whereas the on-resonant probability maintains a constant value of 0.58. Therefore, the TPA probability excited by a laser pulse with a π-phase step scan can be reduced to 58%. The TPA probability normalized by the initial TL pulse is regarded as 100%. As the phase step position is set at a central frequency of 10 353 cm^{-1}, the sign of $E(\omega)E(\omega_{fg}-\omega)$ for all other spectral components are the same, and the TPA probability is equal to that of the TL pulse.

As a Pr^{3+} ion is doped in a crystal, the energy level of $^1G_4$ shifts within hundreds of wave-numbers. For example, the energy level of $^1G_4$ changes within the range of 9 700 to 10 200 cm^{-1}, influenced by the crystal electric field in the PrP_5O_{14} crystal[23]. TPA peaks were calculated with the corresponding intermediate energy levels, as shown in Fig. 4. The peak values are always larger than 8.7 and can reach a maximum value of 15.2 as the intermediate energy level reaches 10 136 cm^{-1}.

As a Pr^{3+} ion is doped in a crystal, the energy levels become wider, influenced by the surrounding crystal electric field. In this case, the Pr^{3+} ion was considered to have a certain absorption bandwidth. The resonant TPA proba-

Fig. 1. Sketches of the energy levels of (a) a Pr^{3+} ion and (b) a Pr^{3+} ion in a crystal.
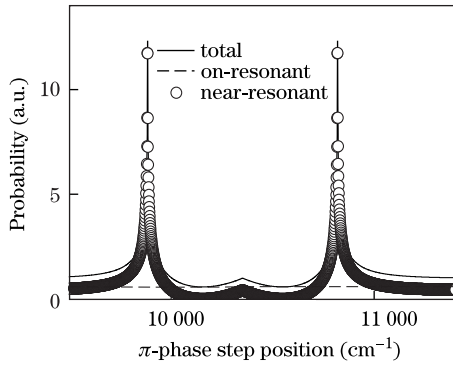
Fig. 3. Resonant TPA probability of a Pr^{3+} ion as well as on-resonant and near-resonant TPA intensities.
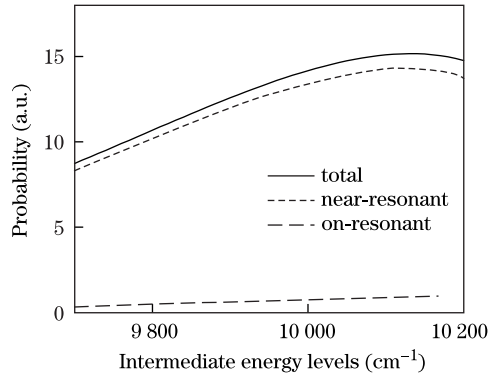

Fig. 4. Total TPA probability and the on-resonant and near-resonant parts of a Pr^{3+} ion with different intermediate energy levels.
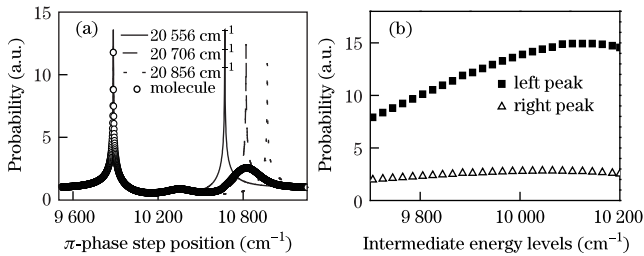

Fig. 5. (a) TPA probability of a Pr^{3+} ion with a certain absorption bandwidth as a function of the π-phase step positions and (b) intermediate energy levels.

bility is proportional to the overlap integral of the absorption spectrum $G(\omega_a)$ and the individual TPA probability. TPA probability is approximated by

$$S_2 = \int_{-\infty}^{\infty} G(\omega_a) \Big| \mathrm{i}\pi E(\omega_{ig}) E(\omega_{fg} - \omega_{ig})$$

$$+ \mathfrak{G} \int_{-\infty}^{\infty} \frac{E(\omega)E(\omega_{fg} - \omega)}{\omega_{ig} - \omega} \mathrm{d}\omega \Big|^2 \mathrm{d}\omega_a. \qquad (3)$$

The absorption band is set as a Gaussian shape, i.e., $G(\omega_a) = Ae^{-2(\omega_a - \omega_{fg})^2/\Delta \omega_1^2}$, where $\Delta \omega_l$ represents the absorption bandwidth of the final state $|f\rangle$. The UCL bandwidth of a Pr^{3+} ion is usually 3 to 5 nm, and $\Delta \omega_l$ is set at 160 cm^{-1} (4.08 nm) in the following calculation.

The TPA probability normalized by the TL pulse as a function of π-phase step positions is shown in Fig. 5(a).

Under this condition, one peak reaches 11.9, and the other peak reaches only 2.6. These results are very different from the ion system shown in Fig. 3. To understand the physical mechanisms, the TPA probability was calculated with the energy levels of the final states at 20 556, 20 706, and 20 856 cm^{-1}, respectively. For different final state levels, one resonant frequency is maintained at the same position for the same intermediate state. However, the other resonant frequency changes with the final state levels. Therefore, the right TPA peak for the molecular system becomes lower and wider.

The effect of intermediate level shift on the TPA peaks in a crystal is shown in Fig. 5(b). The left peak reaches a maximum of 14.9 at an intermediate energy level of 10 125 cm^{-1}, whereas the right peak reaches a maximum of 2.82 at an energy level of 10 065 cm^{-1}. The TPA probability of a Pr^{3+} ion is similar to that in a crystal.

In conclusion, the resonant TPA probability of a Pr^{3+} ion is theoretically demonstrated to be enhanced by a factor of 12.3 using the π-phase step scanning of femtosecond laser pulses, whereas the laser intensity of the shaped pulse is reduced to 37% of the initial TL pulse. Moreover, the absorption bandwidth of the final states and the shift of the intermediate energy level greatly affect the coherent features.

References

1. F. Wang and X. G. Liu, Chem. Soc. Rev. **38,** 976 (2009).
2. S. V. Eliseeva and J.-C. Bünzli, Chem. Soc. Rev. **39,** 189 (2010).
3. J.-C. Bünzli and C. Piguet, Chem. Soc. Rev. **34,** 1048 (2005).
4. M. Haase and H. Schäfer, Angew. Chem. Int. Ed. **50,** 5808 (2011).
5. C. Zhang, H. P. Zhou, L. Y. Liao, W. Feng, W. Sun, Z. X. Li, C. H. Xu, C. J. Fang, L. D. Sun, Y. W. Zhang, and C. H. Yan, Adv. Mater. **22,** 633 (2010).
6. S. Nicolas, M. Laroche, S. Girard, R. Moncorgé, Y. Guyot, M. F. Joubert, E. Descroix, and A. G. Petrosyan, J. Phys. Condens. Matter. **11,** 7937 (1999).
7. P. Xie and T. R. Gosnell, Opt. Lett. **20,** 1014 (1995).
8. P. T. Diallo, P. Boutinaud, and R. Mahiou, J. Alloys Comp. **341,** 139 (2002).
9. M. Malinowski, C. Garapon, M. F. Joubert, and B. Jacquier, J. Phys. Condens. Matter. **7,** 199 (1995).
10. P. A. Rodnyi, S. B. Mikhirin, P. Dorenbos, E. Kolk, C. W. E. Van Eijk, A. P. Vink, and A. G. Avanesov, Opt. Commun. **204,** 237 (2002).
11. H. T. Chen, R. Lian, M. Yin, L. R. Lou, W. P. Zhang, S. D. Xia, and J.-C. Krupa, J. Phys. Condens. Matter. **13,** 1151 (2001).
12. G. S. Macial, R. B. Guimarães, P. G. Batteto, I. C. S. Carvalho, and N. Rakov, Opt. Mater. **31,** 1735 (2009).
13. A. S. Oliveira, E. A. Gouveia, M. T. Araujo, and A. S. Gouveia-Neto, J. Appl. Phys. **87,** 4274 (2000).
14. S. A. Zhang, C. H. Lu, J. H. Shi, T. Q. Jia, Z. G. Wang,

and Z. R. Sun, Phys. Rev. A **84,** 013408 (2011).

15. M. Leibscher, I. S. Averbukh, and H. Rabitz, Phys. Rev. A **69,** 013402 (2004).

16. S. A. Malinovskaya, P. H. Bucksbaum, and P. R. Berman, Phys. Rev. A **69,** 013801 (2004).

17. S. A. Zhang, J. H. Shi, H. Zhang, T. Q. Jia, Z. G. Wang, and Z. R. Sun, Phys. Rev. A **82,** 043841 (2010).

18. A. M. Weiner, Rev. Sci. Instrum. **71,** 1929 (2000).

19. Y. Silberberg, Annu. Rev. Phys. Chem. **60,** 277 (2009).

20. D. Meshulach and Y. Silberberg, Phys. Rev. A **60,** 1287 (1999).

21. N. Dudovich, B. Dayan, S. Faeder, and Y. Silberberg, Phys. Rev. Lett. **86**, 47 (2001).

22. C. Brif, R. Chakrabarti, and H. Rabitz, New J. Phys. **12,** 075008 (2010).

23. S. Y. Zhang, *Spectroscopy of Rare Earth Ions-Spectral Property and Spectral Theory,* (in Chinese) (Science Press, Beijing, 2008).